

## A Composite Analysis of the Boundary Layer Accompanying a Tropical Squall Line

RICHARD H. JOHNSON AND MELVILLE E. NICHOLLS

*Department of Atmospheric Science, Colorado State University, Fort Collins, 80523*

(Manuscript received 18 June 1982, in final form 17 September 1982)

### ABSTRACT

Rawinsonde data from the GARP Atlantic Tropical Experiment (GATE) have been used to prepare a composite of the boundary layer associated with a tropical squall line on 12 September 1974. Soundings from fifteen GATE ships have been composited with respect to the center of the squall radar echo, as determined by Gamache and Houze (1982), for a 9-hour period during which the squall system was approximately in steady-state moving to the southwest at  $13.5 \text{ m s}^{-1}$ . Particular emphasis is given to the modified boundary layer or wake that trails the leading edge of the squall system.

Immediately behind the  $\sim 200 \text{ km}$  wide squall line to a distance of  $\sim 100 \text{ km}$  exists a very cool, stable layer of air several hundred meters deep just above the ocean surface. This region is followed by a shallow mixed layer  $\sim 100 \text{ m}$  deep which gradually increases to  $\sim 500 \text{ m}$  (a depth characteristic of undisturbed regions) at distances behind the line ranging from  $500 \text{ km}$  on the northwest side to  $\sim 300 \text{ km}$  on the southeast side. Surface temperatures and specific humidities within the squall wake are as low as  $4^\circ\text{C}$  and  $3 \text{ g kg}^{-1}$  below the surrounding environmental values.

Composites of wind, surface pressure, temperature, specific humidity, moist static energy, stability atop the mixed layer inversion, and fluxes of sensible and latent heat have been computed and are displayed relative to the squall center. The shallowest mixed layer depths coincide with the surface wind diffluence center located beneath the northwest portion of the mesoscale precipitating anvil cloud trailing the squall line. The composite observations provide a coherent, three-dimensional view of a tropical squall boundary layer which should prove valuable for models of squall wake recovery.

### 1. Introduction

The modification of the planetary boundary layer by downdrafts from deep, precipitating convective systems presents a formidable problem for large-scale numerical weather prediction. In particular, convective parameterization theories, if they are to properly incorporate important effects of cumulus clouds, must take into account the significant transformation of the boundary layer by downdrafts (Betts, 1976; Johnson, 1981; Barnes and Garstang, 1982, and others). Progress toward achieving a better understanding of the interaction between cumulus ( $\sim 1\text{--}10 \text{ km}$ ) and mesoscale ( $\sim 100 \text{ km}$ ) convection and the atmospheric boundary layer has been aided by a number of field programs during the past decade or so, one of the most extensive of which was the 1974 GARP Atlantic Tropical Experiment (GATE). This paper reports on observations taken from GATE that provide a three-dimensional view of the significant modification of the boundary layer accompanying a tropical squall line.

Cumulonimbus downdrafts with their associated strong winds and cool air outflow at the surface can locally increase the surface sensible and latent heat fluxes over tropical oceans by an order of magnitude or more. The collective effect of many tropical convective systems is sufficiently important to enhance

tropical oceanic surface exchanges above those determined from mean tradewind conditions on very large scales (Garstang, 1967). Within the tropical eastern Atlantic region during GATE, downdraft-modified boundary layers or "wakes" accompanying precipitating convective systems were found on the average to cover approximately 30% of the total area (Gaynor and Mandics, 1978; Gaynor and Ropelewski, 1979). Characteristically, in these wakes, cool downdraft air from cumulonimbus convection spreads over a region considerably larger than the clouds themselves (Zipser, 1977a; Simpson and van Helvoirt, 1980), effectively stabilizing the boundary layer near the cold air source and producing shallow, 100–300 m deep mixed layers over large areas which, following the disturbed conditions, recover only slowly over a period of 2–10 h (Houze, 1977; Zipser, 1977a; Augstein, 1978; Gaynor and Mandics, 1978; Fitzjarrald and Garstang, 1981a,b; Johnson, 1981). Frequently, associated with commonly observed mesoscale convective systems in GATE (Leary and Houze, 1979a), warm, dry mesoscale downdrafts in the lower troposphere are observed to cap the shallow cool air near the surface, thereby delaying the recovery of the boundary layer to its undisturbed state (Zipser, 1969, 1977a; Houze, 1977). These warm, dry mesoscale downdrafts are associated with mesoscale anvil cloud systems (Houze, 1977) and are distinctly different

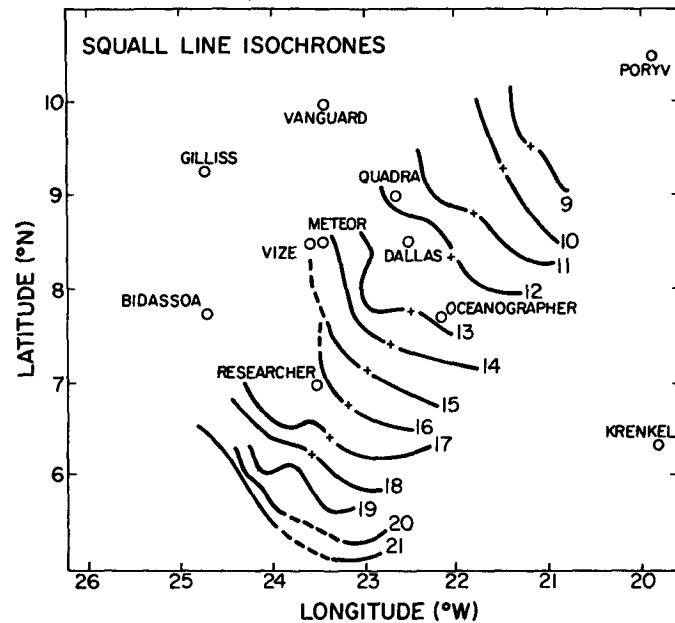


FIG. 1. Isochrone analysis of leading edge of squall line for the period 0900–2100 GMT 12 September 1974 (redrafted from Gamache and Houze, 1982). Crosses mark the center position of the squall. Ship positions are indicated.

from the cool, moist convective-scale downdrafts that spread out over the ocean surface. Often the convective-scale downdraft systems can, through concentrated low-level convergence at their outer edges or intersection with other downdrafts, generate new convective cells (Warner *et al.*, 1980).

The present study has been motivated by the recent work of Gamache and Houze (1982), who have obtained, by a rawinsonde compositing procedure, a remarkably coherent description of the three-dimensional structure of a squall line on 12 September 1974 of GATE. A similar analysis, though not a composite, has recently been carried out by Chen *et al.* (1980). Gamache and Houze (1982) selected a 9-hour period during which the radar structure of the squall on this day was approximately in steady-state and composited GATE ship array soundings relative to the center of the squall radar echo. In our study we extend this composite using rawinsonde data to carry out a detailed investigation of the boundary layer accompanying the squall.

As noted in a review article by Houze and Betts (1981), a considerable number of authors have investigated the squall on this date. Several of these studies have concentrated on the wake recovery. Zipser (1977a) has analyzed surface streamline, thermodynamic and pressure changes associated with the squall passage across the ship array, and examined the recovery of the mixed layer in the trailing wake region using a one-dimensional mixed-layer jump model. Fitzjarrald and Garstang (1981a,b) also studied the wake recovery for the 12 September squall

using data from ship-based tethered instrumentations in their analysis and a jump model for the mixed layer.

Our work differs from these previous boundary layer studies in several respects: 1) primarily ship rawinsonde data are used in the analysis, and 2) boundary layer data are composited relative to the squall to derive a three-dimensional view of its structure. This observational paper forms the basis for heat and moisture budget and modeling studies of the wake recovery which are in progress.

## 2. Observational data and analysis procedures

The primary data used in this study are from the GATE A/B and C-Scale rawinsonde archive obtained from the World Data Center A (Asheville, NC). The observations are from an array of fifteen ships, eleven of which are shown in Fig. 1. The four that are not shown in this figure, but which are used to some extent in the subsequent analyses, complete an outer hexagonal array, the A/B-scale array (containing the *Poryv* and *Krenkel*), with its center at the *Vize*. The rawinsonde data are from ships of five different countries, and consequently various balloons and tracking instrumentation systems and launching and calibration procedures were used (Reeves, 1978). The final validated data set used in this study provides observations of meteorological variables at 5 hPa (mb) intervals. However, the actual vertical resolution of the raw sounding data is not 5 hPa in each instance. Information contained in Reeves (1978) and in the doc-

umentation accompanying the sounding data indicates that the effective vertical resolution of data from the ships *Researcher*, *Gilliss*, *Dallas*, *Oceanographer*, *Quadra*, *Bidassoa* and *Meteor* were variable, but less than 5 hPa. Temperature and humidity contact spacing for the *Vanguard* was such that  $\sim 10$ – $20$  hPa vertical resolution in the lowest 1–2 km was achieved. Sounding data from the Soviet ships *Vize*, *Poryv*, *Krenkel*, and the four other outer hexagon ships not shown in Fig. 1 were determined by mandatory and significant level criteria. Standard levels in the boundary layer were at 1000 hPa, 200, 300, 500 and 600 m. Significant levels were assigned in such a way that linear interpolation between any two adjacent levels in the final sounding would not lead to errors in reported data greater than 1)  $1^\circ\text{C}$  in temperature, 2) 15% in relative humidity and 3)  $5\text{ m s}^{-1}$  in speed or  $10^\circ$  in direction for the wind.

In some instances, the quality of the rawinsonde data at the lowest levels (say, below 500 m) is degraded by factors such as difficulty in initially locking in with transmitter signals, initial mechanical adjustments following launch, etc. These factors obviously contributed on some occasions to a poor sampling of the boundary layer. However, there are a number of reasons to believe that the rawinsonde accuracy is sufficient for the purposes of this study. Reeves *et al.* (1976) found, in an intercomparison study between the 2 hPa vertical resolution BLIS [Boundary Layer Instrument System, Wylie and Ropelewski (1980)] tethered data and rawinsonde data, that agreement between the two systems was generally good (temperature differences  $\sim 1^\circ\text{C}$ , wind speed/direction differences  $\sim 1\text{ m s}^{-1}/15^\circ$ ). In several instances, however, large differences in wind were noted below 950 hPa, probably due to rawinsonde tracking errors at low levels. The study by Fitzjarrald and Garstang (1981a) of wake recovery indicates that rawinsonde data compare favorably with Boundary Layer Instrumentation System (BLIS) data in defining the mixed layer structure. The analyses carried out in our study also support the use of the GATE rawinsonde data to determine gross boundary layer features (e.g., mixed layer depth).

During the period of our composite analysis (0900–1800 GMT 12 September 1974), soundings at 3-hourly intervals were obtained from most of the 15 ships. Hourly positions of the leading edge of the squall radar echo (taken from the paper of Gamache and Houze, 1982) are shown in Fig. 1 for the period 0900 to 2100 GMT. During this time the squall line moved southwestward across the region at an average speed of  $13.5\text{ m s}^{-1}$ . Estimated center positions of the squall line at each hour are indicated by crosses. The reader is referred to Gamache and Houze (1982) for details regarding the radar analysis and compositing procedures. A figure similar to Fig. 1 is presented in Zipser (1977a).

Two components of the squall radar echo have been identified by Gamache and Houze using ship-based weather radars: 1) the squall line itself, and 2) the post-squall anvil region. The former feature refers to the cumulonimbus convection on the leading edge of the squall system. The squall line has a movement that is at times characterized by discrete propagation that takes the form of new growth of convective cells out in advance of old ones, while old ones to the rear weaken (Houze, 1977). The post-squall anvil region refers to the nearly continuous stratiform cloud system of mesoscale ( $\sim 200\text{ km}$ ) dimension trailing the squall line (Houze, 1977; Zipser, 1977a). The average boundaries of these squall components will be outlined in subsequent figures.

Since data have been composited over a 9-hour period, the analysis of the sea level pressures includes a correction for the semi-diurnal pressure oscillation, which has an amplitude in this region of  $\sim 2.5\text{ hPa}$  (e.g., Zipser, 1977a).

Mixed layer depths have been determined for ship soundings that show an approximately well-mixed structure in potential temperature or dry static energy  $s$  ( $\equiv c_p T + gz$ ). Both profiles of  $s$  and specific humidity  $q$  were used to subjectively estimate the depth of the mixed layer by locating positions of abrupt changes in lapse rates (e.g., Esbensen, 1975).

Surface sensible and latent heat fluxes  $S_0$  and  $LE_0$ , respectively, have been determined using ship boom data from the *Gilliss*, *Dallas*, *Researcher* and *Oceanographer* and the bulk aerodynamic relationships

$$S_0 = \bar{\rho} c_p C_h \bar{u}_{10} (\bar{\theta}_0 - \bar{\theta}_{10}), \quad (1)$$

$$E_0 = \bar{\rho} C_e \bar{u}_{10} (\bar{q}_0 - \bar{q}_{10}), \quad (2)$$

where  $\bar{\rho}$  is the mean density,  $c_p$  specific heat for dry air,  $C_h$  the bulk transfer coefficient for sensible heat,  $C_e$  the bulk transfer coefficient for water vapor,  $E_0$  the surface evaporation, and  $\bar{u}_{10}$  the mean wind speed at 10 m. The subscripts 0 and 10 refer to values at the ocean surface and 10 m level, respectively, and overbar refers to a time average (10 min means are used in our analyses). The recommended values for  $C_h$  and  $C_e$  for both undisturbed and disturbed conditions are  $(1.6 \pm 0.5) \times 10^{-3}$  and  $(1.4 \pm 0.4) \times 10^{-3}$ , respectively (U.S. GATE Workshop, 1977). A correction term that reflects the dependence of  $c_p$  on specific humidity has been added to (1) in some recent studies (e.g., Reinking and Barnes, 1981) based on an analysis by Brook (1978). More recently, however, Frank and Emmitt (1981) and Businger (1982) have argued that Brook's correction is in error and, therefore, we have neglected it.

### 3. Composite results

#### a. Mixed-layer depth and vertical structure

Out of 53 ship rawinsonde soundings from the 15 ships available for the 9-h period of this study, 36, or

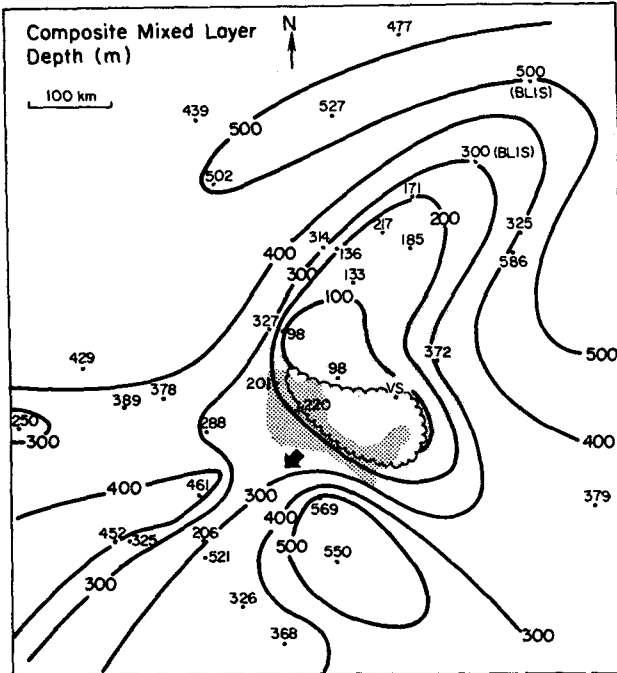


FIG. 2. Composite mixed layer depth (m). Actual depths at sounding positions are indicated; VS denotes a very stable lapse rate in the lowest several 100 m at indicated sounding position. Scalped curve encloses estimated area of very stable boundary layer. Squall line is moving in direction of arrow at  $13.5 \text{ m s}^{-1}$ . Dark and light shaded regions denote squall-line (convective echo) and anvil (stratiform echo) regions, respectively. BLIS observations are from tethered sondes aboard the *Dallas*.

68%, show evidence of a mixed layer structure. This percentage, as might be expected given the disturbed conditions during the period, is somewhat less than the  $\sim 80\%$  frequency of well-mixed layers found by Fitzjarrald and Garstang (1981a) using BLIS data for all of GATE.

A subjective analysis of the mixed layer depths for the composite squall is shown in Fig. 2. Depths at the individual sounding positions are indicated. The analysis does not fit perfectly with the data (also true for subsequent figures), but this is to be expected for several reasons: 1) during the composite period, the squall radar echo structure is not exactly in steady state and its speed is somewhat irregular and 2) small-scale ( $\leq 10 \text{ km}$ ) inhomogeneities in the mixed layer are probably being sampled by the soundings, inhomogeneities which are known to exist both in the regions of recovery from disturbed conditions (Fitzjarrald and Garstang, 1981a, Fig. 6) and in fair weather areas (Barnes *et al.*, 1980). The squall line echo area defined by Gamache and Houze (1982) is shown in the figure by dark shading, and post-squall anvil (the outer contour of the anvil precipitation shown in their Fig. 4b) by light shading.

Of primary significance in Fig. 2 is the wake or

extensive area with a suppressed mixed layer behind the squall line. Mixed layers in the wake are significantly shallower than the reported mean for undisturbed GATE conditions (Brümmer, 1978; Gaynor and Ropelewski, 1979; Nicholls and LeMone, 1980; Fitzjarrald and Garstang, 1981a). The scalloped area in Fig. 2 is an estimate of the extent of the very cool, stable boundary layer following the squall where mixed layers, if they exist at all, have depths smaller than that resolvable by the sounding data ( $\leq 50 \text{ m}$ ). The large extent of the wake to  $\sim 500 \text{ km}$  behind the squall leading edge has been discussed by others (Houze, 1977; Zipser, 1977a; Fitzjarrald and Garstang, 1981a,b). However, this composite view shows that there are important asymmetries in its structure about a centerline perpendicular to the squall. As will be discussed later, this asymmetry can probably be attributed to mesoscale asymmetries 1) in the composite flow field in the wake region, and/or 2) the intensity of deep convection in the squall line itself.

Another important feature of the composite mixed layer analysis is a region of shallow mixed layers in advance of and approximately perpendicular to the squall. This feature is most likely associated with a line of cumulonimbus convection that existed preceding the squall (Zipser, 1977a,b; Gamache and Houze, 1982). This pre-existing line had an important effect on the convective intensity in the squall (Zipser, 1977b), and perhaps, as a consequence, on the asymmetric structure of the squall wake (to be discussed later).

Profiles of dry static energy  $s$  for all soundings with well-mixed structures that were located within and in the immediate vicinity of the squall system are shown in Fig. 3. Positions of individual soundings can be determined by matching mixed layer depths indicated at the top of each curve with values plotted in Fig. 2. Ahead of and immediately northwest and southeast of the squall and its wake, mixed layers  $\sim 500 \text{ m}$  deep are observed. In the trailing wake, a significantly cooled and suppressed mixed layer is found which recovers toward an undisturbed structure well to the rear. The average distances from the squall's leading edge of the first two clusters of plotted soundings in the wake are indicated in Fig. 3. There is a significant variation in the distances from the leading edge for soundings in the last group since they are distributed about the periphery of the wake. As can be seen by noting the equivalent times after squall passage (in parentheses in Fig. 3), the mixed layer recovery illustrated here is quite consistent with that shown by Fitzjarrald and Garstang (1981a, Fig. 6) using the high resolution *Dallas* BLIS data (i.e., a long recovery period of  $\sim 7\text{--}10 \text{ h}$ ). An important point revealed by this composite study however, is that the horizontal extent of the wake recovery suggested by the BLIS data alone for this squall system is an overestimate for the wake as a whole, because

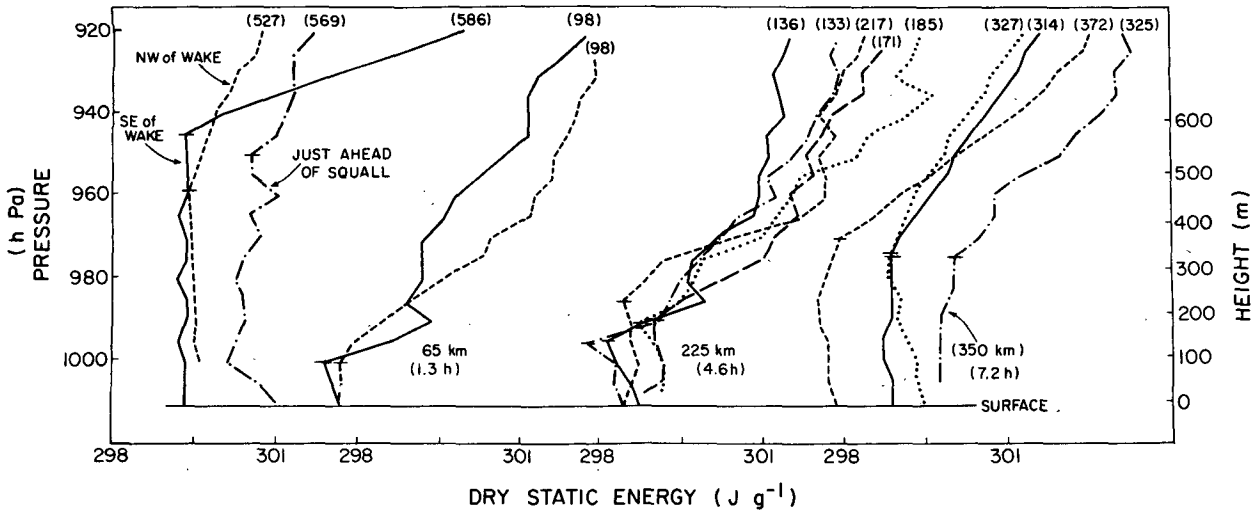


FIG. 3. Profiles of dry static energy  $s$  within and in the immediate vicinity of the squall system. Mixed-layer depths (m) indicated at tops of curves can be used to locate sounding position relative to squall by referring to Fig. 2. The middle two clusters of soundings are positioned within the wake at average distances of 65 and 225 km behind the squall leading edge (corresponding to 1.3 and 4.6 h, respectively). The last sounding on the right is in the wake and is 350 km or 7.2 h behind the leading edge.

of the asymmetry in the wake structure. That is, much more rapid recovery occurs in the southeast portion of the wake.

Significant drying atop the wake mixed layer (Zipser, 1977a) is seen in individual wake soundings (Fig. 4). These profiles are again consistent with those presented for this squall by Fitzjarrald and Garstang (1981a) using BLIS data.

*b. Wind fields*

The composite surface flow field has been presented and discussed by Gamache and Houze (1982). Our surface streamline analysis (Fig. 5) is virtually the same as theirs, showing 1) a confluence line per-

pendicular to and in advance of the squall line; 2) a convergence line coincident with the leading edge of the squall; and 3) a strong diffluence center beneath the mesoscale anvil cloud. When comparing figures shown in this study to those in Gamache and Houze, the reader should note that the latter authors have presented fields in a rotated coordinate system aligned with the squall direction of motion.

Also shown in Fig. 5 are the composite mixed layer depths. The shallowest mixed layers in the wake are observed near the surface diffluence center. Inspection of the plotted winds in Fig. 5 (and the isotach analysis in Fig. 5a of Gamache and Houze) indicate this region is also a center of strong surface divergence and, consequently, low-level subsidence. The close

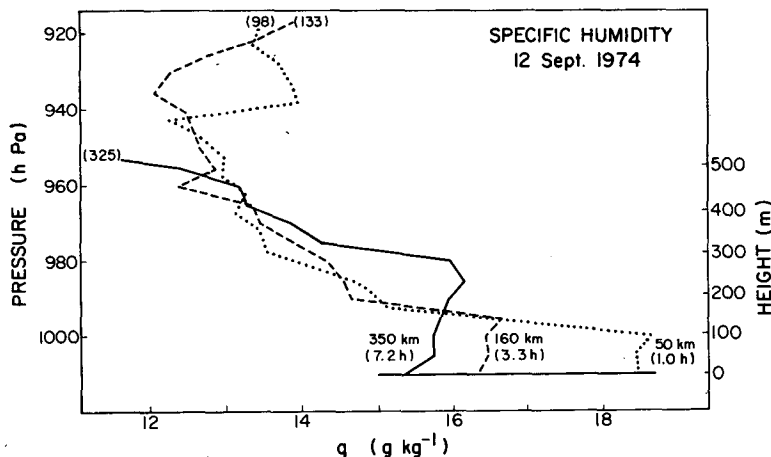


FIG. 4. Profiles of specific humidity for three wake soundings. Notation as in Fig. 3.

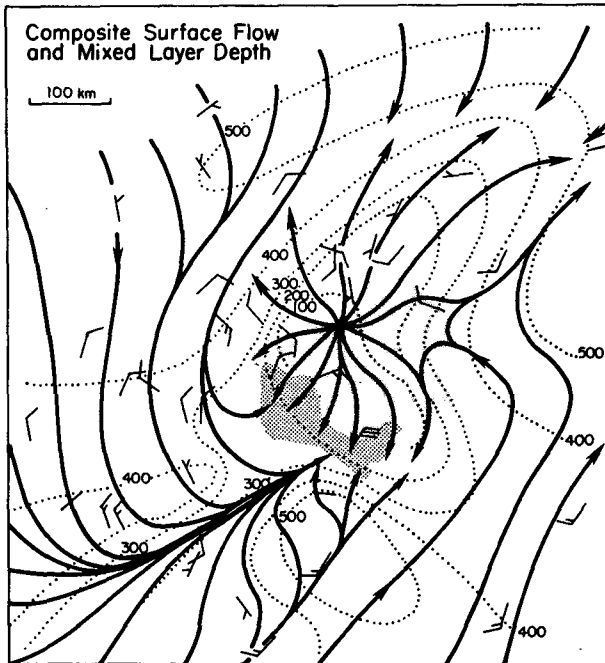


FIG. 5. Composite surface streamline flow and mixed layer depth (m). One full barb =  $5 \text{ m s}^{-1}$ , one half barb =  $2.5 \text{ m s}^{-1}$ .

coincidence of the mixed layer depth minimum with the suggested position of strongest sinking is qualitatively consistent with simple mixed layer theory, although other factors, e.g., the horizontal variation of the surface fluxes, must be considered. Simple mixed-layer models have been applied by Zipser (1977a) and Fitzjarrald and Garstang (1981b) to this case and have qualitatively done well in explaining the prolonged nature of the wake recovery. Work is in progress to carry out a more detailed, three-dimensional modeling analysis of the wake recovery using the composited data reported in this study.

The more rapid recovery of the mixed layer in the southeast portion of the squall wake (Fig. 5) can be at least partly attributed to the considerably weaker surface divergence (and hence subsidence) that is evident from the streamline analysis in that region and from Fig. 5c of Gamache and Houze (1982). Furthermore, Zipser (1977b) points out that convection in the southern portion of the squall line was considerably weaker than that near its center where the squall intersected the pre-existing convective line. The weaker convection in the southern part may have produced weaker downdrafts and a weaker trailing anvil system (as is suggested in Gamache and Houze, 1982, Fig. 4a), thereby allowing for a more rapid recovery of the boundary layer in that region.

In a rather detailed analysis of the motion field at individual times for the 12 September squall, Chen *et al.* (1980) found a significant vertical variation in the wake-flow field in the lower troposphere. Gamache and Houze (1982) show that at 850 hPa the

surface diffluence center is overlaid by strong ( $\sim 10\text{--}20 \text{ m s}^{-1}$ ) northeasterly winds. At 970 hPa the diffluence center is still evident (Fig. 6), but is displaced northward by  $\sim 100 \text{ km}$ . The significant variation of the wind in the lowest levels indicates that estimates of vertical velocities based *solely* on surface winds for use in mixed layer computations may lead to considerable errors.

### c. Thermodynamic and pressure fields

In the subsequent discussion we will focus primarily on the structure of the squall-line system and omit comments on the convective band ahead of the squall, even though its existence is evident in most of the composite fields.

Accompanying the passage of the squall is a sudden drop in the temperature of  $\sim 4^\circ\text{C}$  with the coolest surface air  $\sim 50 \text{ km}$  behind the leading edge of the squall (Fig. 7). As discussed by Houze (1977) and Zipser (1977a), it takes a considerable length of time,  $\sim 6\text{--}8 \text{ h}$  (corresponding to  $\sim 300\text{--}400 \text{ km}$ ), for the surface air to warm to pre-squall conditions. The surface specific humidity depression is delayed however, and does not reach a minimum until 3–4 h (150–200 km) after the squall passage (Fig. 8). This phenomenon, as noted by Zipser (1977a), is also common to squall lines in the eastern Pacific Ocean. The maximum depression of specific humidity at the surface below ambient values is  $3\text{--}4 \text{ g kg}^{-1}$ .

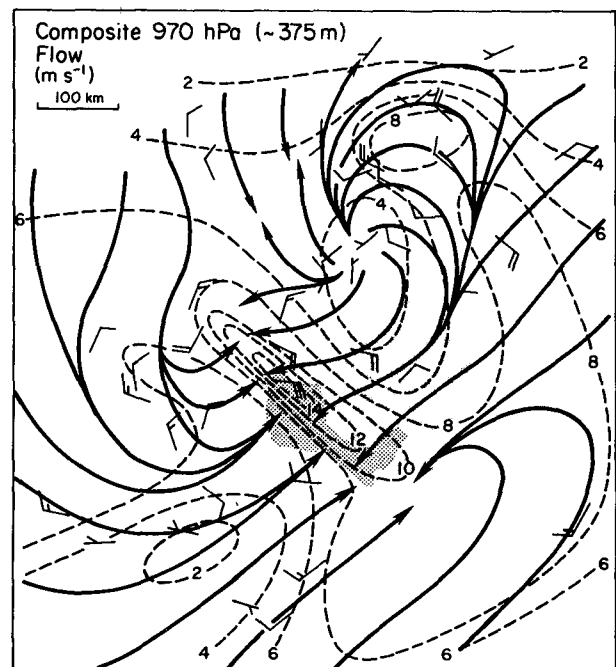


FIG. 6. Composite flow at 970 hPa ( $\sim 375 \text{ m}$ ). Dashed lines are isotachs ( $\text{m s}^{-1}$ ). Several observations of 2100 GMT have been added in this analysis to better delineate the flow behind the trailing anvil.

The lag in the surface drying (reduction in  $q$ ) behind the surface cooling has been discussed by Zipser (1977a) and Fitzjarrald and Garstang (1981b). The latter authors attribute the drying and its coincidence with the period of surface warming to the occurrence of rapid deepening of the mixed layer and entrainment of drier air from above. Comparison of Figs. 2, 7 and 8 indicates that Fitzjarrald and Garstang's explanation may be valid since the lowest values of  $q$  occur in a region of rapid mixed layer recovery near the center of the wake. However, the importance of a three-dimensional analysis to an accurate assessment of the key processes in wake recovery is clearly evident when one considers that Fitzjarrald and Garstang's interpretation is based on the BLIS tether-sonde record in the northwest portion of the wake, whose track indicates a considerably slower recovery (Fig. 2). Our observations suggest that accurate budget studies and modeling of the wake recovery must consider all components of its horizontal structure.

The composite surface relative humidity (not shown) indicates values >90–95% in an area approximately corresponding to the squall echo with steadily decreasing values to the rear reaching ~80% about 200–300 km behind the leading edge (e.g., see *Oceanographer* time series in Fig. 12 of Houze, 1977). Thus, while there is an actual minimum in  $q$  in the wake, the relative humidity decreases monotonically from values just below saturation in the squall line echo region to environmental values well to the rear.

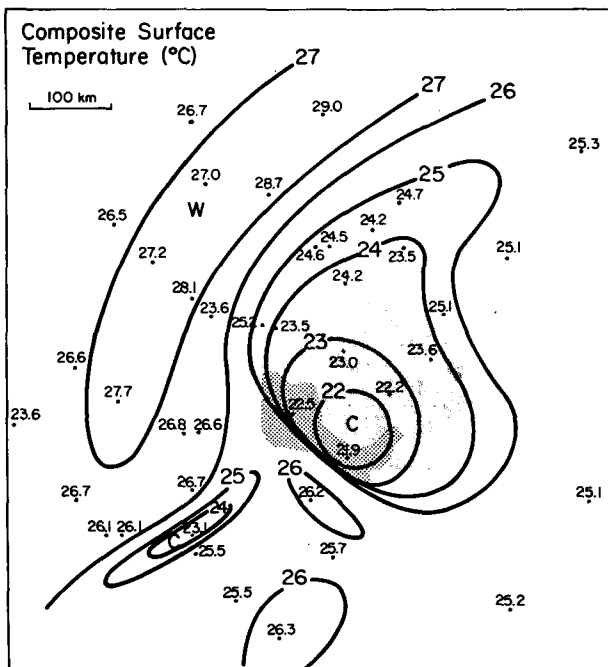


FIG. 7. Composite surface temperature at ship deck or ~10 m level (°C).

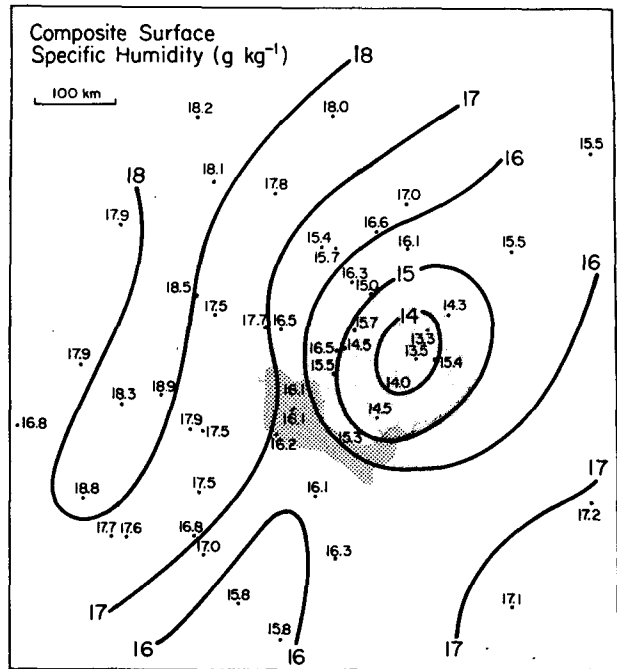


FIG. 8. Composite surface specific humidity ( $g\ kg^{-1}$ ).

The surface pressure field, with the semi-diurnal component removed, depicts a mesohigh accompanying the squall line and mesolow centered ~500 km to the rear of the system (Fig. 9). The mesohigh, which can probably be attributed to the cold, saturated air and large liquid water contents in the squall downdrafts (Zipser, 1977a), is relatively small in horizontal extent (<100 km) compared to the mesolow (~500 km dimension). The mesolow is centered approximately twice as far behind the squall leading edge as the surface specific-humidity depression center, but coincides almost precisely with the position of a warm anomaly at 900 hPa (Fig. 10). This warm lower troposphere, which is produced by mesoscale subsidence beneath the mesoscale anvil (Houze, 1977; Zipser, 1977a; Brown, 1979), accounts hydrostatically for the existence of the mesolow to the rear of the squall (Zipser, 1977a). Similar mesolows beneath mesoscale anvils are observed associated with midlatitude squall lines or thunderstorm complexes (Fujita, 1963; Hoxit *et al.*, 1976), and similar mechanisms for producing such mesolows at midlatitudes are suggested from the modeling study of Fritsch and Chappell (1980). The lower troposphere is also dry in the mesoscale downdraft region, as indicated in Fig. 11. Relative humidities below 60% at 900 hPa cover a large area and the thermodynamic structure portrayed in Figs. 10 and 11 is consistent with the “onion”- or “diamond”-shaped temperature and dew point soundings that are frequently seen in the anvil portion of tropical squall systems (Zipser, 1977a). Specific humidities (not shown) near the center of the dry region at 900 hPa

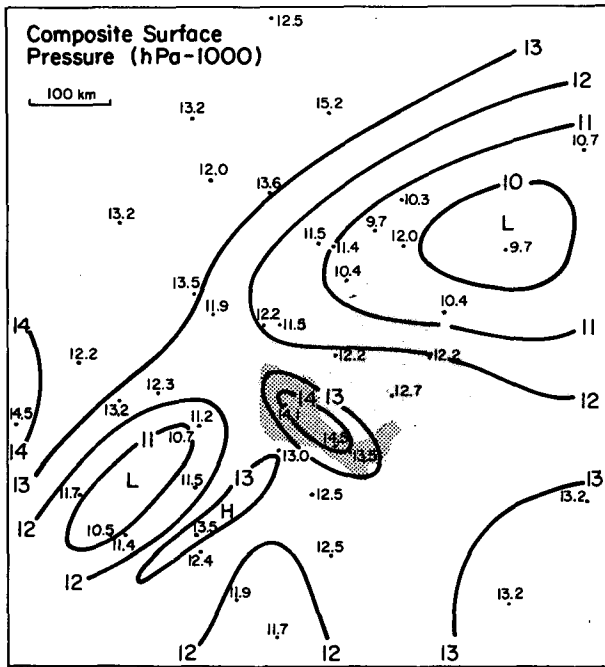


FIG. 9. Composite surface pressure (minus 1000 hPa). Semi-diurnal pressure oscillation has been removed.

are as low as  $9 \text{ g kg}^{-1}$ , or approximately  $5 \text{ g kg}^{-1}$  below values observed in and adjacent to the squall system radar echo. Similar structures in mesoscale downdrafts in convection near Borneo have been recently observed and reported on by Johnson and Kriete (1982).

At the surface there is a considerable reduction in the moist static energy  $h = c_p T + gz + Lq$ , following the squall passage (Fig. 12). If  $h$  is considered to be conservative and air from the cool saturated squall downdrafts, which is felt to comprise the shallow surface wake (Zipser, 1977a), has its origins in the mid-to lower troposphere, then pre-squall soundings (not shown) indicate that the downdraft air must have come from at least as high as 700 hPa or  $\sim 3 \text{ km}$ . The computed relative flow field for the squall and mesoscale anvil by Gamache and Houze (1982) suggests a level  $\sim 4 \text{ km}$  above the surface to the rear of the anvil may also be a possible source region for the low- $h$  air at the surface (their Fig. 16a). This relative inflow from the rear is indicated in the studies by Houze (1977), Zipser (1977a) and Johnson and Kriete (1982). However, whether or not this air within the anvil downdraft circulation is entrained into the mixed layer and transported down to the surface is questionable (Zipser, 1977a). Soundings within the anvil region indicate values of  $h$  in the mid-to lower troposphere that are low enough to account for the low- $h$  surface air even if an additional lowering of  $h$  by the nonconservative effect of hydrometeor melting just below the freezing level (Leary and Houze, 1979b; Chen *et al.*, 1980) is not taken into account.

*d. Surface fluxes*

The strong winds immediately behind the leading edge of the squall line produce a sudden increase in the instantaneous surface fluxes of sensible and latent

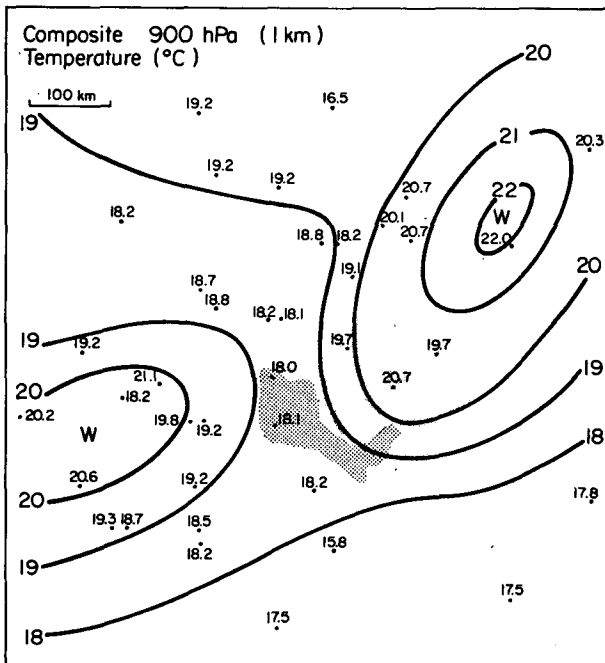


FIG. 10. Composite 900 hPa ( $\sim 1 \text{ km}$ ) temperature ( $^{\circ}\text{C}$ ).

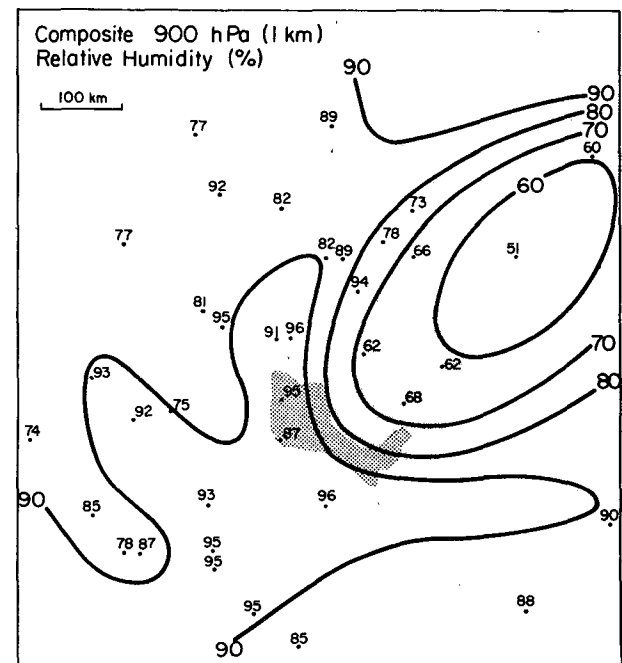


FIG. 11. Composite 900 hPa ( $\sim 1 \text{ km}$ ) relative humidity (%).



heat. Composite analyses of surface sensible and latent heat fluxes determined by (1) and (2) are shown in Figs. 13 and 14. The hourly positions of the ships *Gilliss*, *Dallas*, *Researcher* and *Oceanographer*, which had boom data, as well as the *Meteor*, which had sea surface temperature data, are indicated in the figures. For comparison, examples of estimated GATE mean values of sensible and latent heat fluxes for undisturbed conditions are  $10 \text{ W m}^{-2}$  and  $90 \text{ W m}^{-2}$ , respectively (e.g., Thompson *et al.*, 1979; Reinking and Barnes, 1981).

To a distance of  $\sim 100 \text{ km}$  behind the leading edge of the squall line the sensible heat flux increases over undisturbed values by a factor  $\sim 5$  (in an area-averaged sense) as a result of higher surface winds and reduced air temperatures. A composite analysis of the sea surface temperatures (not shown) shows no systematic variation across the squall. However, the amplitude of any fluctuation, if of the same magnitude as that found by Reed and Lewis (1979) accompanying the passage of synoptic-scale African easterly waves ( $\leq 0.4^\circ\text{C}$ ), is probably sufficiently small to preclude detection for a single case. It is clear that it is primarily the surface cooling by convective downdrafts that contributes to enhanced sensible heat fluxes over most of the anvil region, considering the relatively light winds at the surface beneath much of the anvil region (Fig. 5), and the small fluctuation in sea surface temperatures compared to the 10 m air temperature changes (Fig. 7). Gaynor and Ropelewski (1979) find an average increase of 2.5 times in the sensible heat flux in GATE convective wakes, a factor

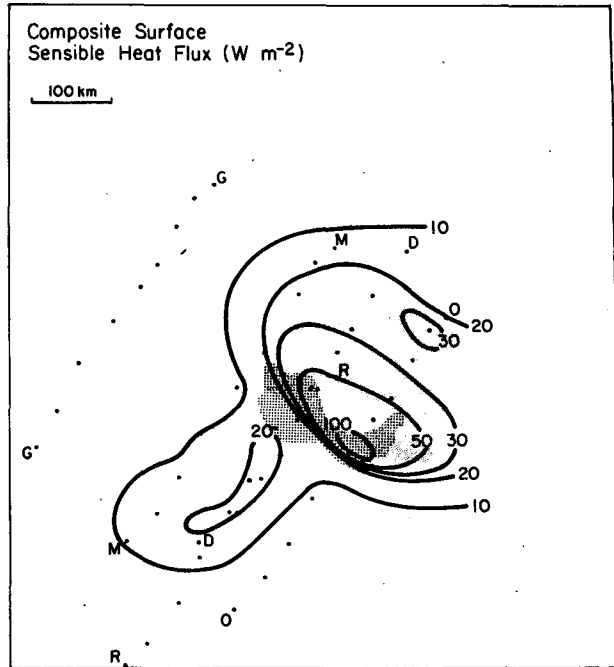


FIG. 13. Composite surface sensible heat flux ( $\text{W m}^{-2}$ ). Hourly positions of *Gilliss* (G), *Meteor* (M), *Dallas* (D), *Researcher* (R), and *Oceanographer* (O) are indicated by dots.

generally consistent with the results here when considering averages over the entire squall wake.

The latent heat flux (Fig. 14) also shows a sharp increase at the squall line, primarily due to the strong

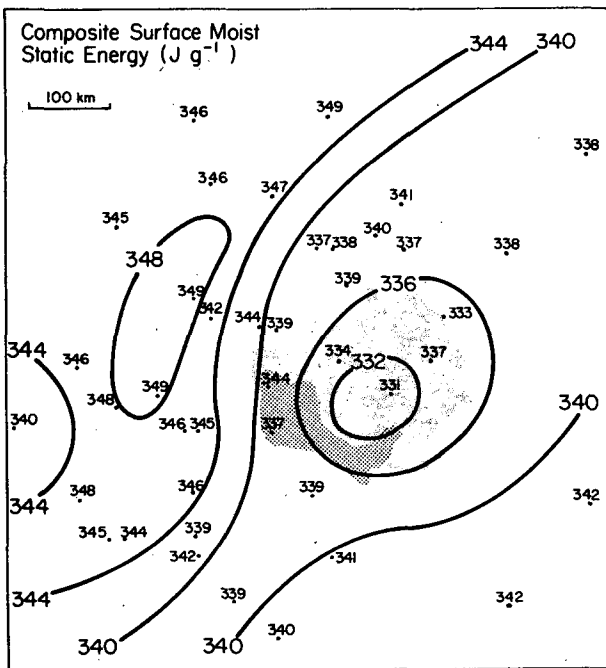


FIG. 12. Composite surface moist static energy ( $\text{J g}^{-1}$ ).

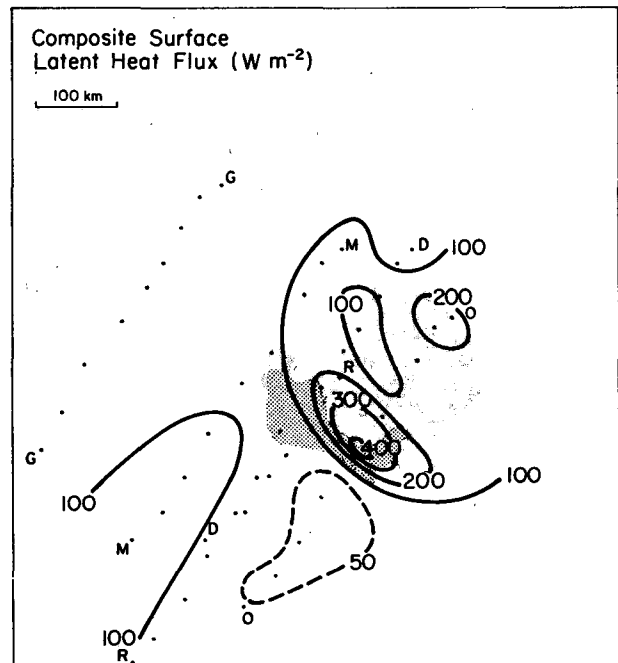


FIG. 14. As in Fig. 13, except for composite surface latent heat flux ( $\text{W m}^{-2}$ ).

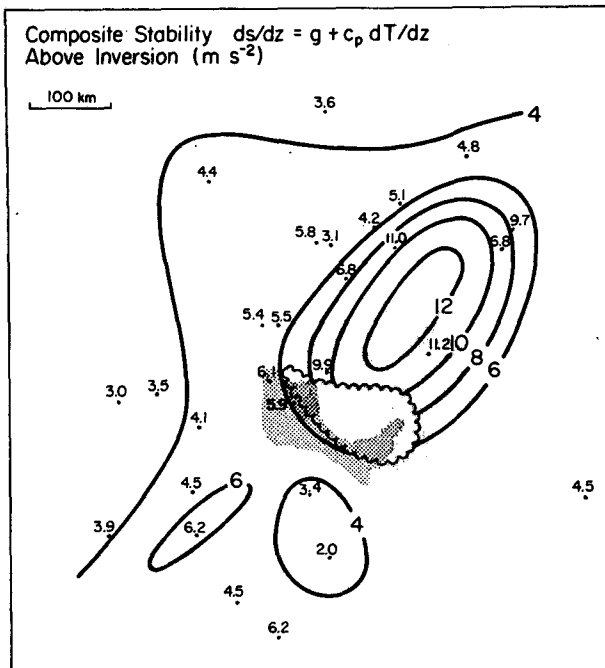


FIG. 15. Composite stability atop the mixed layer inversion ( $m s^{-2}$ ). Scalloped curve encloses estimated area of very stable boundary layer as in Fig. 2.

winds there, with a wake-average increase of  $\sim 2$  times more than that for undisturbed conditions. The enhancement of the latent heat flux over the majority of the wake area can largely be attributed to significant surface drying (Fig. 8). This finding for the squall differs from the general conclusions by Gaynor and Ropelewski (1979) who find the latent heat flux slightly smaller in GATE wakes as a whole, primarily due to lighter surface winds. This difference between the 12 September squall and GATE wakes in general can probably be accounted for by the fact that strong squalls, like the one studied here, were rare events, whereas the more common convective systems, while also producing wakes, produced considerably weaker modifications, i.e., a smaller reduction of  $q$ , of the surface air (Zipser *et al.*, 1981).

#### e. Stability atop the mixed layer inversion

One of the most dramatic effects of the post-squall anvil system is the subsidence warming and drying that occurs in the lower troposphere over a large area. This feature has already been discussed in terms of temperature and relative humidity fields at 900 hPa. Gamache and Houze (1982) find that the mesoscale subsidence reaches a maximum amplitude of  $\sim -10$   $cm s^{-1}$  near 850–900 hPa. As might be expected, this sinking motion has a significant stabilizing effect on the lower troposphere.

Normally, above the mixed layer there exists a transition layer  $\sim 100$  m deep that is more stable than

the free atmosphere above (see Fitzjarrald and Garstang, 1981a for mean structure based on BLIS data). The stability atop the transition layer or mixed layer inversion has an important effect on the time evolution of the mixed layer depth (Zipser, 1977a; Fitzjarrald and Garstang, 1981b; Johnson, 1981). The more stable the atmosphere is above the mixed layer, the more slowly it will grow (other conditions being the same). Accurate predictions of mixed layer recovery require accurate specification of the lapse rate above the inversion. In Fig. 15 the composite stability  $ds/dz$  above the mixed layer inversion is presented. This lapse rate is determined above the transition layer from individual sounding plots where the transition layer depth has been subjectively estimated. In those cases where a transition layer is not evident from the rawinsonde data, the lapse rate in the free atmosphere is determined beginning  $\sim 100$  m above the mixed layer top (based on Fitzjarrald and Garstang's (1981a) mean transition layer depth estimate).

The analysis in Fig. 15 shows that within the downdraft wake region the stability above the mixed layer inversion increases by approximately a factor of three and the region of a stabilized lower troposphere is extensive ( $\sim 500$  km). Of course, the results shown here are consistent with the analysis of considerable warming at 900 hPa described in Fig. 10. Ahead of the squall there is a small region of more unstable lapse rates, perhaps reflecting the effects of mesoscale lifting along its leading edge.

#### 4. Summary and discussion

A study of the modification and recovery of the boundary layer following the passage of a tropical squall line through the GATE ship array on 12 September 1974 has been carried out. Rawinsonde data from 15 GATE ships have been composited with respect to the center of the squall radar echo, as determined by Gamache and Houze (1982), for a 9-hour period during which the squall system was approximately in a steady state moving to the southwest at  $13.5$   $m s^{-1}$ . Soundings at 3-hour intervals having effective vertical resolutions ranging from  $\leq 5$  hPa to 10–20 hPa were used to determine the mixed layer depth and to document the thermodynamic and flow characteristics of the boundary layer wake accompanying the squall. The mixed layer properties determined from balloon soundings compare quite favorably with those obtained using high resolution tethered sonde (BLIS) data from GATE (Fitzjarrald and Garstang, 1981a).

The findings of this study are consistent with and complementary to previous investigations of the squall wake on 12 September (Zipser, 1977a; Fitzjarrald and Garstang, 1981a), but the results here add another dimension to the previous analyses. By compositing the rawinsonde data, the horizontal structure

of the boundary layer within and around the squall system has been deduced.

Immediately behind the  $\sim 200$  km wide squall line to a distance of  $\sim 100$  km exists a very cool, stable layer of air near the ocean surface. This region is followed by a shallow mixed layer  $\sim 100$  m deep which gradually increases to  $\sim 500$  m (a depth characteristic of undisturbed regions) at distances behind the line (normal to it) ranging from  $\sim 500$  km on the northwest side to  $\sim 300$  km on the southeast side (Fig. 2). The more rapid recovery of the squall boundary layer wake in the southeast portion is consistent with: 1) the implied weaker subsidence in this region (from surface streamline analyses, Fig. 5) than in the northwest portion of the wake; and 2) the weaker intensity of convection in the southeast portion of the squall. The shallowest mixed layer depths coincide with the surface wind diffluence center located beneath the northwest portion of the mesoscale precipitating anvil cloud trailing the squall line (Gamache and Houze, 1982).

Composites of surface pressure, temperature, specific humidity, moist static energy and fluxes of sensible and latent heat have been computed and are displayed relative to the squall center. A mesohigh of  $\sim 100$  km dimension directly accompanies the squall line itself, with a much larger ( $\sim 500$  km) mesolow centered approximately 500 km behind the leading edge. Composite temperature fields in the lower troposphere indicate the mesolow can be accounted for hydrostatically by a large area of warm air within the mesoscale downdraft beneath the anvil cloud (Zipser, 1977a; Gamache and Houze, 1982). This warm, subsiding air produces considerably increased stability atop the mixed layer inversion in this region and along with the increased subsidence in this region, very likely contributes to the slow wake mixed-layer recovery.

The results of this study have important implications pertaining to the development of tropical mesoscale systems as well as, perhaps, tropical cyclones. As recently stressed by Johnson (1981), Barnes and Garstang (1982) and others, tropical mesoscale convection can significantly modify the boundary layer and suppress the mixed layer (below the lifting condensation level of the surface air) over very large areas and for a considerable length of time. This suppression can discourage new convection over the region of modified air. As Barnes and Garstang pointed out, the entire process may account for the rarity of the event of intensification of a tropical disturbance into a tropical cyclone. The results of this study also suggest that a proper handling of convective downdrafts and wakes will be of paramount importance in achieving a successful scheme of convective parameterization in large-scale prediction models.

The compositing procedure used in this study has yielded a reasonably coherent picture of the 12 Sep-

tember squall boundary layer, just as it has been equally successful for the cloud layer above (Gamache and Houze, 1982). The consistency between the various fields has motivated a detailed modeling investigation of the recovery of the squall wake, the results of which will be reported on later. Many of the approximations introduced in previous modeling studies will not be necessary with the three-dimensional fields, including vertical motion, that are now available.

*Acknowledgments.* We appreciate the information on squall center positions provided to us by Mr. John Gamache and Professor Robert Houze of the University of Washington prior to their publication. Professor Colleen Leary, Texas Tech University, sent helpful information on the vertical resolution of GATE soundings. Thanks go to Machel Sandfort for typing the manuscript. This work has been supported by the National Science Foundation, Division of Atmospheric Sciences, Global Atmospheric Research Program, under Grant ATM-8015347.

#### REFERENCES

- Augstein, E., 1978: The atmospheric boundary layer over the tropical oceans. *Meteorology Over the Tropical Oceans*, Roy. Meteor. Soc., 73-103.
- Barnes, G., and M. Garstang, 1982: Subcloud layer energies of precipitating convection. *Mon. Wea. Rev.*, **110**, 102-117.
- , G. D. Emmitt, B. Brümmer, M. A. LeMone and S. Nicholls, 1980: The structure of a fair weather boundary layer based on the results of several measurement strategies. *Mon. Wea. Rev.*, **108**, 349-364.
- Betts, A. K., 1976: The thermodynamic transformation of the tropical subcloud layer by precipitation and downdrafts. *J. Atmos. Sci.*, **33**, 1008-1020.
- Brook, R. R., 1978: The influence of water vapour fluctuations on turbulent fluxes. *Bound.-Layer Meteor.*, **15**, 481-487.
- Brown, J. M., 1979: Mesoscale unsaturated downdrafts driven by rainfall evaporation: A numerical study. *J. Atmos. Sci.*, **36**, 313-338.
- Brümmer, B., 1978: Mass and energy budgets of a 1 km high atmospheric box over the GATE C-scale triangle during undisturbed and disturbed weather conditions. *J. Atmos. Sci.*, **35**, 997-1011.
- Businger, J. A., 1982: The fluxes of specific enthalpy, sensible heat and latent heat near the earth's surface. *J. Atmos. Sci.*, **39**, 1889-1892.
- Chen, Y.-L., E. J. Zipser, G. M. Barnes and E. J. Szoke, 1980: Mesoscale structure of the 12 September squall line case in GATE. Paper presented at 13th Tech. Conf. Hurricanes and Tropical Meteorology, Miami Beach, Amer. Meteor. Soc.
- Esbensen, S., 1975: An analysis of subcloud-layer heat and moisture budgets in the western Atlantic trades. *J. Atmos. Sci.*, **32**, 1921-1933.
- Fitzjarrald, D. R., and M. Garstang, 1981a: Vertical structure of the tropical boundary layer. *Mon. Wea. Rev.*, **109**, 1512-1526.
- , and —, 1981b: Boundary-layer growth over the tropical ocean. *Mon. Wea. Rev.*, **109**, 1762-1772.
- Frank, W. M., and G. D. Emmitt, 1981: Computation of vertical total energy fluxes in a moist atmosphere. *Bound.-Layer Meteor.*, **21**, 223-230.
- Fritsch, J. M., and C. F. Chappell, 1980: Numerical prediction of

- convectively driven mesoscale pressure systems. Part II: Mesoscale model. *J. Atmos. Sci.*, **37**, 1734–1762.
- Fujita, T., 1963: *Analytical Mesometeorology: A Review. Meteor. Monogr.*, No. 27, Amer. Meteor. Soc., 77–125.
- Gamache, J. F., and R. A. Houze, Jr., 1982: Mesoscale air motions associated with a tropical squall line. *Mon. Wea. Rev.*, **110**, 118–135.
- Garstang, M., 1967: Sensible and latent heat exchange in low-latitude synoptic-scale systems. *Tellus*, **19**, 492–509.
- Gaynor, J. E., and P. A. Mandics, 1978: Analysis of the tropical marine boundary layer during GATE using acoustic sounder data. *Mon. Wea. Rev.*, **106**, 223–232.
- , and C. F. Ropelewski, 1979: Analysis of the convectively modified GATE boundary layer using *in situ* and acoustic sounder data. *Mon. Wea. Rev.*, **107**, 985–993.
- Houze, R. A., Jr., 1977: Structure and dynamics of a tropical squall-line system observed during GATE. *Mon. Wea. Rev.*, **105**, 1540–1567.
- , and A. K. Betts, 1981: Convection in GATE. *Rev. Geophys. Space Phys.*, **19**, 541–576.
- Hoxit, L. R., C. F. Chappell and J. M. Fritsch, 1976: Formation of mesolows or pressure troughs in advance of cumulonimbus clouds. *Mon. Wea. Rev.*, **104**, 1419–1428.
- Johnson, R. H., 1981: Large-scale effects of deep convection on the GATE tropical boundary layer. *J. Atmos. Sci.*, **38**, 2399–2413.
- , and D. C. Kriete, 1982: Thermodynamic and circulation characteristics of winter monsoon tropical mesoscale convection. *Mon. Wea. Rev.*, **110**, 1898–1911.
- Leary, C. A., and R. A. Houze, 1979a: The structure and evolution of convection in a tropical cloud cluster. *J. Atmos. Sci.*, **36**, 437–457.
- , and —, 1979b: Melting and evaporation of hydrometeors in precipitation from the anvil clouds of deep tropical convection. *J. Atmos. Sci.*, **36**, 669–679.
- Nicholls, S., and M. LeMone, 1980: The fair weather boundary layer in GATE: The relationship of subcloud fluxes and structure to the distribution and enhancement of cumulus clouds. *J. Atmos. Sci.*, **37**, 2051–2067.
- Reed, R. J., and R. M. Lewis, 1979: Response of upper ocean temperatures to diurnal and synoptic-scale variations of meteorological parameters in the GATE B-scale area. *Deep Sea Res.*, **25**, 99–114.
- Reeves, R. W., 1978: GATE Convective Subprogram Data Center: Final Report on Rawinsonde Data Validation. NOAA Tech. Rep. EDS 29, 31 pp. [NTIS PB-281-861].
- , S. Williams, E. Rasmusson, D. Acheson and T. Carpenter, 1976: GATE convection sub-program data center—Analysis of rawinsonde intercomparison data. NOAA Tech. Rep. EDS 20, 75 pp. [NTIS PB-264 815].
- Reinking, R. F., and G. Barnes, 1981: A comparison of tropical oceanic heat fluxes determined by airborne eddy correlation and shipboard bulk aerodynamic techniques. *Bound.-Layer Meteor.*, **20**, 353–370.
- Simpson, J., and G. van Helvoirt, 1980: GATE cloud-subcloud layer interactions examined using a three-dimensional cumulus model. *Contrib. Atmos. Phys.*, **53**, 106–134.
- Thompson, R. M., Jr., S. W. Payne, E. E. Recker and R. J. Reed, 1979: Structure and properties of synoptic-scale wave disturbances in intertropical convergence zone of the eastern Atlantic. *J. Atmos. Sci.*, **36**, 53–72.
- U.S. GATE Central Program Workshop, 1977: NCAR Rep., 723 pp.
- Warner, C., J. Simpson, G. van Helvoirt, D. W. Martin, D. Suchman and G. L. Austin, 1980: Deep convection on day 261 of GATE. *Mon. Wea. Rev.*, **108**, 169–194.
- Wylie, D. P., and C. F. Ropelewski, 1980: The GATE Boundary Layer Instrumentation System (BLIS). *Bull. Amer. Meteor. Soc.*, **61**, 1002–1011.
- Zipser, E. J., 1969: The role of organized unsaturated convective downdrafts in the structure and rapid decay of an equatorial disturbance. *J. Appl. Meteor.*, **8**, 799–814.
- , 1977a: Mesoscale and convective-scale downdrafts as distinct components of squall line structure. *Mon. Wea. Rev.*, **105**, 1568–1589.
- , 1977b: 12 September case study. Report of the U.S. GATE Central Program Workshop, NCAR, 339–341.
- , R. J. Meitin and M. A. LeMone, 1981: Mesoscale motion fields associated with a slowly moving GATE convective band. *J. Atmos. Sci.*, **38**, 1725–1750.